American Mineralogist, Volume 82, pages 1–7, 1997

Si-Al order and the $I\bar{1}$-$I2/c$ structural phase transition in synthetic $CaAl_2Si_2O_8$-$SrAl_2Si_2O_8$ feldspar: A ^{29}Si MAS-NMR spectroscopic study

BRIAN L. PHILLIPS,[1] MARTIN D. MCGUINN,[2] AND SIMON A.T. REDFERN[2,*]

[1]Division of Materials Science and Engineering, University of California, Davis, California 95616, U.S.A.
[2]Department of Geology, University of Manchester, Manchester M13 9PL, U.K.

ABSTRACT

We present ^{29}Si MAS-NMR spectroscopic data for a series of synthetic feldspar samples along the join $CaAl_2Si_2O_8$-$SrAl_2Si_2O_8$, from which the composition dependence and coupling of order parameters describing Si-Al order and the triclinic-monoclinic displacive transition were determined. Spectra of $SrAl_2Si_2O_8$ contain narrow peaks for the two crystallographic Si sites, plus additional peaks for Si having three and two Al nearest neighbors, indicating the presence of approximately 0.14 Al-O-Al linkages per formula unit and a value of $\sigma = 0.93$ for the short-range order parameter. For the triclinic feldspar samples, short-range Si-Al order increases continuously with Sr content from $\sigma = 0.89(3)$ for $CaAl_2Si_2O_8$ to 0.97(1) for $Sr_{0.80}Ca_{0.20}Al_2Si_2O_8$ but then decreases discontinuously to 0.93(2) for the monoclinic samples, $Sr_{0.85}Ca_{0.15}Al_2Si_2O_8$ to $SrAl_2Si_2O_8$. The variation of peak positions with composition is consistent with a structural phase transition near $Sr_{0.85}Ca_{0.15}Al_2Si_2O_8$ from $I\bar{1}$ to $I2/c$. The order parameter for this displacive transition is reflected by the chemical shift of the T1mz crystallographic site, and its composition dependence gives an order-parameter critical exponent of $\beta = 0.49(2)$, indicating classical second-order behavior.

INTRODUCTION

A complete solid solution exists for feldspar between the compositions $CaAl_2Si_2O_8$ (anorthite) and $SrAl_2Si_2O_8$, although at ambient conditions the symmetry changes from $P\bar{1}$ for pure anorthite to $I\bar{1}$ for intermediate compositions to $I2/c$ for $SrAl_2Si_2O_8$. Recently, McGuinn and Redfern (1994) have shown that the variation in the lattice parameters across this compositional join corresponds to a ferroelastic triclinic-to-monoclinic phase transition from space group $I\bar{1}$ to $I2/c$ near the composition $Sr_{0.86}Ca_{0.14}Al_2Si_2O_8$ at room temperature. Some questions remained from the XRD study regarding the variation in the state of Si-Al order with composition and the coupling of the ferroelastic strains to those resulting from Si-Al disorder, providing the motivation for the present work.

Of particular interest is the possibility that the $I\bar{1}$-$I2/c$ displacive transition may couple strongly to changes in Si-Al order. The $I\bar{1}$-$I2/c$ transition is thought to be truly ferroelastic, driven by softening of the critical elastic constants (Dove and Redfern 1997). Because the monoclinic and triclinic phases are both body centered, they may both entertain varying degrees of Si-Al order (completely disordered equivalents have symmetry $C2/m$ and $C\bar{1}$). Tribaudino et al. (1993) investigated the effect of changing long-range Si-Al order on the $I2/c$-$I\bar{1}$ transition and showed that the critical temperature (T_c) was lowered for more disordered samples. Furthermore, they suggested that samples with a lower long-range order parameter, Q_{od}, showed a transition that tended toward being first order at more calcic compositions. Room-temperature TEM observations of an intermediate strontium-calcium feldspar have revealed a change of microstructure as annealing time (and therefore Q_{od}) increases (Tribaudino et al. 1995). The microstructure of samples annealed for short periods contains only Carlsbad growth twins, characteristic of monoclinic feldspar. Longer annealing produces more ordered samples that display higher temperatures for the monoclinic-triclinic transition. As the sample becomes triclinic, a ferroelastic microstructure develops. When the degree of ordering produced a sample for which T_c was close to room-temperature, grains of both monoclinic and triclinic material were observed, apparently indicating the first-order nature of the transition. Although the possibility of chemical inhomogeneity within the samples was not addressed in their study, this factor may also be expected to make the transition apparently first order.

McGuinn and Redfern (1994) noted that the two triclinic strains e_4 and e_6 (corresponding essentially to changes in cos α^* and cos γ, respectively) do not behave identically below the phase transition. Although e_4 may be thought of as the primary order parameter and behaves according to a mean-field second-order process, e_6 does not scale in the same way with composition below the transition, increasing more rapidly with increasing Ca

*Present address: Department of Earth Sciences, University of Cambridge, Downing Street, Cambridge CB2 3EQ, U.K.

0003–004X/97/0102–0001$05.00

content and showing linear-quadratic and higher-order coupling to the order parameter (e_4). The recent results of static lattice simulation of the solid solution by Dove and Redfern (1997) indicate similar nonlinearity between the composition-dependent behaviors of γ and α in the triclinic phase. Here, we wish to determine whether this nonlinearity reflects coupled changes in Q_{od} across the $I\bar{1}$-$I2/c$ displacive transition and have used NMR to investigate both the local distortive order parameter and the local Si-Al order-disorder behavior across the solid solution.

Previous ^{29}Si MAS-NMR spectroscopic studies of anorthite have demonstrated that this technique can provide quantitative information on the extent of short-range Si-Al order (Phillips et al. 1992) and can be used to probe structural changes associated with phase transitions (Phillips and Kirkpatrick 1995). The NMR spectra are insensitive to structural features farther than ~5 Å from the probe nucleus, furnishing structural and configurational data that complement those obtained from diffraction measurements. In this paper we present ^{29}Si MAS-NMR spectroscopic data for the series of synthetic feldspar samples across the $CaAl_2Si_2O_8$-$SrAl_2Si_2O_8$ join studied by McGuinn and Redfern (1994). These spectra display sufficient detail for determination of the degree of local Si-Al order and the variation of the local order parameter for the $I\bar{1}$-$I2/c$ ferroelastic phase transition, confirming the second-order nature of this transition.

Experimental methods

Samples

Feldspar samples with composition $Sr_xCa_{1-x}Al_2Si_2O_8$, $0 \leq x \leq 1$, were prepared from stoichiometric mixtures of $CaCO_3$, $SrCO_3$, Al_2O_3, and SiO_2 by decarbonation at 800 and 1000 °C, followed by crystallization at 1500 °C for 72 h. Further details of the synthesis procedure and XRD data for a similar set of samples was given by McGuinn and Redfern (1994). In the present work we refer to samples by their nominal composition as mole percent $SrAl_2Si_2O_8$; for example, Sr20 refers to a feldspar of composition $Sr_{0.20}Ca_{0.80}Al_2Si_2O_8$.

NMR spectroscopy

The ^{29}Si MAS-NMR spectra were recorded at 59.6 MHz with a Chemagnetics CMX-300 spectrometer and MAS sample probe configured for 7.5 mm diameter zirconia rotors. The MAS rate was 5 kHz for all samples. Bloch decays were collected using single-pulse excitation consisting of 90° pulses of 5.5–6.0 μs separated by a recycle delay of 300 s, corresponding approximately to the spin-lattice relaxation time (T_1) for the $SrAl_2Si_2O_8$ sample. These experimental conditions satisfy the Ernst relationship for optimum signal-to-noise ratio while maximizing signal intensity with respect to baseline distortion. Spectra of Sr100 and Sr65, collected with 1000 s recycle delays, show no significant difference with respect to those obtained at 300 s. Each spectrum corresponds to a total accumulation time of 2 d. The data were digitized at 20 kHz, and the first three points of the time-domain data were recalculated by linear prediction prior to Fourier transformation to remove a slight baseline roll. No other filter was applied to the data.

We report the ^{29}Si chemical shifts relative to tetramethylsilane (TMS), but kaolinite was used as an external secondary standard. The kaolinite shows peaks at −90.86 and −91.50 ppm from TMS, and these positions can be determined with a reproducibility better than ±0.02 ppm. Spectra of the secondary reference collected just before and after that of each feldspar sample indicate that the instrument drift over each 2 d data-collection period was <0.04 ppm.

Results and discussion

The ^{29}Si MAS-NMR spectra show large, but mostly continuous changes across the $CaAl_2Si_2O_8$-$SrAl_2Si_2O_8$ series (Fig. 1). Most apparent is a narrowing of the main region of intensity, between −80 and −90 ppm, from three peaks near Sr0, to two peaks with intensity ratio ~2.5:1 from Sr40 to Sr80, and two narrower peaks of approximately equal intensity from Sr85 to Sr100. These changes are consistent with a symmetry change from $I\bar{1}$ for the Ca-rich feldspar, which contains four inequivalent Si sites, to $I2/c$ near $SrAl_2Si_2O_8$ (two Si sites). All the spectra also contain relatively broad peaks at about −5 and −10 ppm from the main peaks that are due to Si with fewer than four Al nearest neighbors (NN), from which the presence of Al-O-Al linkages can be inferred. A slight discontinuity in the spectra appears between Sr80 and Sr85, denoted by a change in the intensity ratio of the two main peaks and, with increasing Sr content, an increase in the intensity of the broad peak at −90 ppm. This compositional break occurs near the critical composition for the monoclinic-to-triclinic transition, $X_c = Sr_{0.86}Ca_{0.14}Al_2Si_2O_8$, previously determined by XRD techniques (McGuinn and Redfern 1994).

The spectrum of the synthetic anorthite (Sr0) closely resembles data presented by Phillips et al. (1992). It contains three main peaks with chemical shifts of −82.4, −85.3, and −89.5 ppm that are nearly identical to those of Si-Al–ordered $P\bar{1}$ anorthite and assigned to the crystallographic sites T1ooi + T1ooo + T2ozo, T2moi + T2ozi + T2moo, and T1mzi + T1mzo, respectively. In addition, there are broad, less intense peaks near −94 and −99 ppm that result from Si environments with <4 Al NN, indicating the presence of some short-range Si-Al disorder. The relative intensity of the peak near −82.4 ppm (32%) is inconsistent with an $I\bar{1}$ framework, which would give peak intensities in multiples of 1/4, and indicates that this sample exhibits local $P\bar{1}$ symmetry.

For Sr100, the ^{29}Si MAS-NMR spectrum contains two well-resolved peaks, at −83.8 and −85.4 ppm, plus broader peaks centered near −90 and −96 ppm. On the basis of the mean Si-O-Al angles from the X-ray structure refinement of Chiari et al. (1975), we assigned the peaks at −83.8 and −85.4 to the crystallographic sites T2z ($\langle\theta\rangle$ = 135.9°) and T1o ($\langle\theta\rangle$ = 137.9°), respectively (Fig. 2).

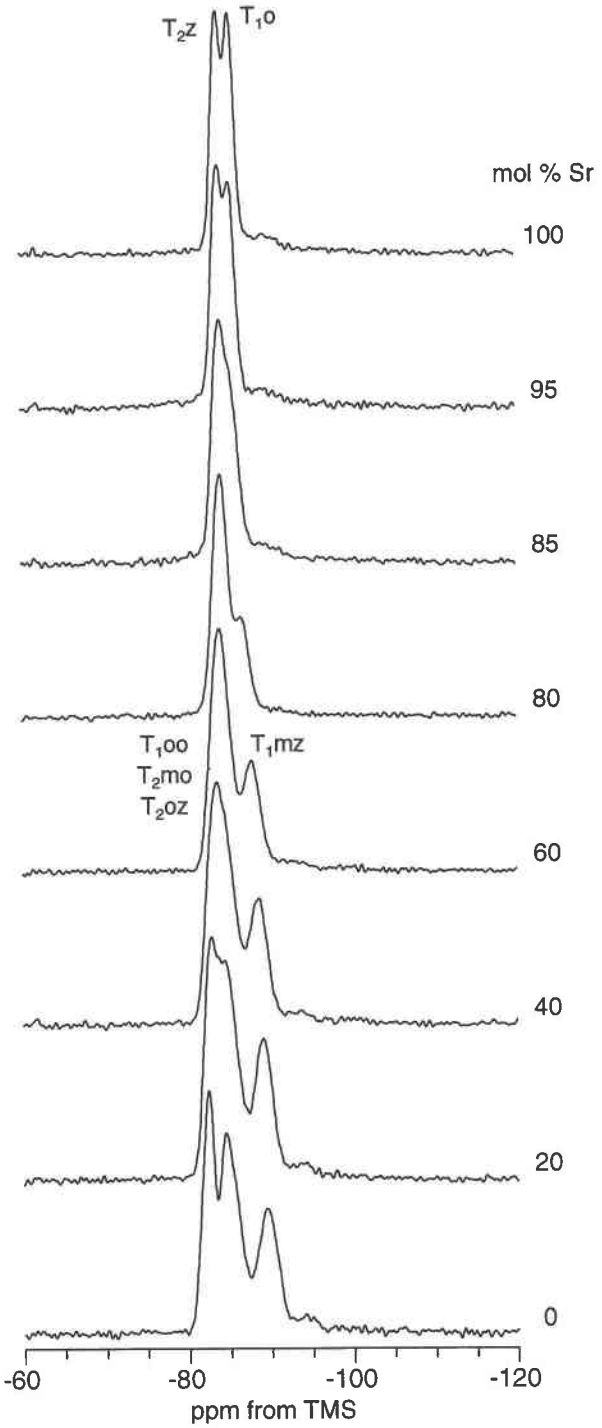

FIGURE 1. The ^{29}Si MAS-NMR spectra of synthetic $(Sr,Ca)Al_2Si_2O_8$ feldspar samples. Pulse width 5.5–6.0 μs (90°), 300 s recycle delay, 500–600 acquisitions. No line broadening was applied to the data.

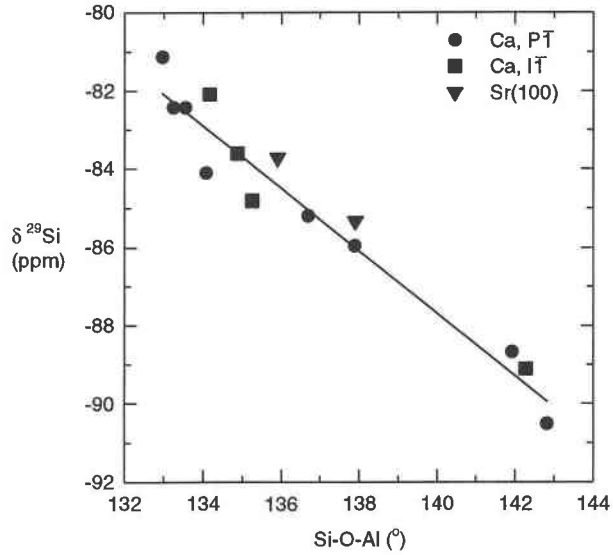

FIGURE 2. Variation of ^{29}Si NMR chemical shift with mean Si-O-Al angle per Si tetrahedron for calcium-strontium feldspar samples. Data for $P\bar{1}$ and $I\bar{1}$ anorthite are from Phillips and Kirkpatrick (1995).

These assignments follow the general trend of more negative chemical shift with increasing mean intertetrahedral angle noted for a wide range of framework aluminosilicates (e.g., Radeglia and Engelhardt 1985), including the $P\bar{1}$ and $I\bar{1}$ phases of anorthite (Phillips and Kirkpatrick 1995).

The spectra of Sr95 and Sr85 appear very similar to that of Sr100, especially with regard to the intensity of the broad peak at −90 ppm. A decrease in the widths of the two main peaks, from about 2.3 to 1.6 ppm (full-width at half-maximum, FWHM) from Sr85 to Sr100, appears to be the principal difference, whereas the chemical shifts of these peaks vary by <0.1 ppm.

The intensity of the broad peak near −90 ppm decreases significantly from Sr85 to Sr80, which suggests an increase in the degree of short-range Si-Al order. But, from Sr0 to Sr80 the spectral changes are continuous, including the movement of the peak for T1mz from −89.5 to −86.7 ppm and the convergence of the sharp peak at −82.4 ppm with that at −85.3 ppm. These peak shifts are related to the monoclinic-to-triclinic symmetry change and are discussed more fully below.

Short-range Si-Al order

A method for determining the state of short-range Si-Al order of anorthite, on the basis of a comparison of the first moment of the ^{29}Si NMR spectrum ($\langle\delta\rangle$) with that of an ordered sample ($\langle\delta\rangle_o$), was presented by Phillips et al. (1992). This procedure gives $N_{Al\text{-}Al}$, the number of Al-O-Al linkages per formula unit (eight O atoms), assuming a constant shift of peak position for each Si NN cation ($\Delta_{Si\text{-}Si} \approx -5 \pm 0.5$ ppm) and Si/Al = 1:

TABLE 1. Peak position for the T1o,T1mz site, intensities of Q^4(3Al) and Q^4(2Al) peaks, and corresponding values of the short-range Si-Al order parameter (σ) for synthetic $Sr_xCa_{1-x}Al_2Si_2O_8$ feldspars

x	$\delta_{T1mz,T1o}$ ($\pm$0.05 ppm)	I_{3Al}	I_{2Al}	σ
0.00	−89.53	n.d.	n.d.	0.89(3)
0.20	−89.03	n.d.	n.d.	n.d.
0.40	−88.48	n.d.	n.d.	n.d.
0.60	−87.77	n.d.	n.d.	n.d.
0.65	−87.53	n.d.	n.d.	n.d.
0.70	−87.23	n.d.	n.d.	n.d.
0.75	−86.96	n.d.	n.d.	n.d.
0.80	−86.65	0.04(1)	0.010(5)	0.97(1)
0.85	−85.37	0.09(2)	0.03(1)	0.93(2)
0.95	−85.42	0.10(2)	0.04(1)	0.92(2)
1.00	−85.42	0.09(2)	0.02(1)	0.93(2)

Note: Chemical shifts are for the T1mz site in the $I\bar{1}$ samples (Sr0–Sr80) and for T1o in the monoclinic samples (Sr85–Sr100); values of σ obtained from Equations 1 and 2 for x = 0.0, otherwise from Equations 3 and 2. Estimated uncertainties in the last digits are given in parentheses; n.d. = not determined.

$$N_{\text{Al-Al}} = \frac{1}{\Delta_{\text{Si-Si}}}(\langle\delta\rangle - \langle\delta\rangle_o) \quad (1)$$

where $\langle\delta\rangle_o$ is considered to be −85.14(10) ppm, the value obtained for the well-ordered Val Pasmeda anorthite. The short-range Si-Al order parameter, σ, is defined to vary from 0 for a random Si-Al distribution to 1 for complete order:

$$\sigma \equiv 1 - \frac{1}{2}N_{\text{Al-Al}}. \quad (2)$$

Note that, in general, σ differs from the long-range order parameter, Q_{od}, which describes the Si-Al occupancies of the crystallographic sites. For reasons of symmetry, σ is expected to vary as the square of Q_{od}, and this has been observed experimentally (Phillips et al. 1992).

For the Sr0 sample of the present study, the first moment ($\langle\delta\rangle$) is −86.2(3) ppm, giving a short-range order parameter of σ = 0.89(3) (Table 1). This value is slightly smaller than that observed previously for samples annealed for a similar period (Phillips et al. 1992), as expected from the higher sintering temperature of the present samples (1500 vs. 1400 °C). Unfortunately, this method for determining σ cannot be applied to the other Ca-rich samples because the average chemical shift for the fully ordered state should vary with composition and cannot be determined from the present data.

In principle, σ can be determined in a similar manner for the Sr-rich samples (Sr85–Sr100) because the peaks for the two crystallographic Si sites are well resolved and their positions do not vary significantly. Therefore, it seems reasonable that the average chemical shift of a fully ordered feldspar at these compositions is given by the mean position of the two narrow peaks: $\langle\delta\rangle_o$ = −84.6 ppm. The first moment does not vary significantly between Sr85 and Sr100 and was found to be −85.7(4) ppm, from which Equations 1 and 2 give a value of σ = 0.89(4). The uncertainties were determined from propagation of spectral noise, but this analysis is also subject to systematic error because of the subjective nature of the phase correction. Extreme care was taken to obtain pure absorption-mode spectra by recalculating the first three data points with a linear prediction algorithm to remove a slight baseline roll and applying a phase correction such that the centerbands and first-order spinning sidebands were in-phase. The resulting spectra contained no systematic deviation from a flat baseline at zero intensity.

Alternatively, the degree of Si-Al order for Sr85–Sr100 can be obtained by simply fitting the spectra with a sum of Gaussian curves: two narrow peaks assigned to the crystallographic sites [Q^4(4Al)] plus broader peaks near −90 and −96 ppm, assigned, respectively, to Q^4(3Al) and Q^4(2Al) Si environments. These spectra also exhibit a tail extending toward more positive chemical shifts, to which we fitted an additional curve, centered near −81 ppm, which contains about 4% of the intensity. The origin of this tail is uncertain, but we assume it results from Q^4(4Al) environments in strained regions. For frameworks in which Si/Al = 1, $N_{\text{Al-Al}}$ equals the average number of Si-O-Si linkages per Si atom (Phillips et al. 1992) and can be determined from

$$N_{\text{Al-Al}} = \sum_{n=0}^{4} (4 - n)\cdot I_n \quad (3)$$

where I_n is the relative intensity of peaks resulting from Si environments with n Al NN cations.

Relative populations of the local Si environments were obtained from partially constrained least-squares fits of the spectra, the results of which are given in Table 1. To obtain physically interpretable results, we found it necessary to constrain the widths of the peaks centered at −90 and −96 ppm. Because of the low signal-to-noise ratio of these peaks, unconstrained fits contain a combination of broad (>10 ppm FWHM) and narrow (<2 ppm) peaks and produce residuals below noise level. Widths of 4–5 ppm (FWHM) give reasonable fits, with no long-period oscillations in the residuals, and restrict overlap of the fitted Q^4(3Al) peak with those resulting from Q^4(4Al) environments. The estimated uncertainties (Table 1) cover the range of intensities that result from varying the widths over this extent. Values of σ obtained by this method, 0.92–0.93 ($\pm$0.02), do not vary significantly from Sr85 to Sr100 and are slightly higher than those obtained from Equations 1 and 2.

Of the remaining samples with intermediate composition, Equation 3 can be applied directly only to Sr80. For this sample, the separation of the Q^4(4Al) peaks (2.5 ppm) is smaller than that between the Q^4(4Al) and Q^4(3Al) peaks, allowing the spectrum to be fitted with four fairly well-resolved peaks [two for Q^4(4Al) and one each for Q^4(3Al) and Q^4(2Al)]. The results show a decrease of σ, from 0.97 to 0.93, with increasing Sr content from Sr80 to Sr85. For the more Ca-rich samples, the Q^4(3Al) peaks resulting from crystallographic sites hav-

ing Q^4(4Al) peaks near −85 ppm (T1oo, T2oz, T2mo) overlap the Q^4(4Al) peak for T1mz (near −90 ppm), preventing accurate determination of peak intensities. However, the spectral changes appear to be continuous from Sr80 to Sr0 (including data not shown in Fig. 1 for Sr65, Sr70, and Sr75), which suggests that the state of short-range order varies smoothly across this compositional range.

For comparison of Si-Al order across the series we prefer the method based on Equation 3 because it is applicable to samples on both sides of the triclinic-monoclinic boundary (Fig. 3). The estimated uncertainties given in Table 1 and Figure 3 include the systematic variations that result from small changes in spectrum processing and phasing, and from the range of assumed peak widths discussed above. These potential systematic errors do not affect our conclusions regarding the relative changes in the degree of Si-Al order across the triclinic-monoclinic boundary. The approximately twofold increase in $N_{\text{Al-Al}}$ from Sr80 to Sr85 and the constant value of σ from Sr85 to Sr100 are obtained as long as the spectra are processed and fit in the same manner, consistent with the trend in the intensity of the peak at −90 ppm evident in the spectra.

The variation in short-range order across the solid solution shows certain similarities with the variation in the γ angle in the same samples (as given by McGuinn and Redfern 1994). The γ angle increases rapidly with increasing Ca content below the critical composition X_c. It is known that γ and e_6 are sensitive to changes in Si-Al order in feldspar (see, for example, Salje et al. 1985). The rapid change in short-range order across the transition boundary (between samples Sr80 and Sr85) reflects the increasing order that is possible in the $I\bar{1}$ phase because of the relaxation of the constraint that γ = 90°. In other words, increasing Si-Al order and increasing e_6 and e_4 are positively coupled in these 2:2 feldspar samples, as they are in albite (Salje et al. 1985). This conclusion accounts for the shift in the transition boundary toward Sr0 for more disordered samples (Tribaudino et al. 1993): Disorder inhibits the development of e_6 and hardens the elastic constant C_{66}, stabilizing the monoclinic structure.

The gradual increase in σ between Sr0 and Sr80 can be explained in similar terms. The lattice-simulation studies of Dove and Redfern (1997) show that Sr substitution for Ca increases γ, with the γ angle rapidly falling to zero at the transition to monoclinic *I*2/*c*. The driving strain for the transition is e_4, and e_6 reflects not only the displacive instability but also the influence of Sr substitution and Si-Al ordering. Because at fixed Q_{od}, γ increases with increasing Sr content, the positive coupling between σ and γ induces an increase in short-range order across the triclinic solid solution with increasing Sr content, as indeed our results show (Fig. 3).

The $I\bar{1}$-*I*2/*c* transition

The most notable changes in the MAS-NMR spectra across the $CaAl_2Si_2O_8$-$SrAl_2Si_2O_8$ series result from the reduction in the number of inequivalent Si sites, from four to two, that accompanies the symmetry change from triclinic for Ca-rich compositions to monoclinic near $SrAl_2Si_2O_8$. On the basis of XRD measurements, McGuinn and Redfern (1994) showed that the structural changes along this join can be described as a ferroelastic structural phase transition from $I\bar{1}$ to *I*2/*c* near the critical composition $X_c = Sr_{0.86}Ca_{0.14}Al_2Si_2O_8$, at room temperature. At this transition, the $I\bar{1}$ framework cation sites related by pseudodiad axes parallel to [010], which have similar Si occupancy factors, become equivalent. Among the Si-rich sites, those labeled T1oo and T1mz converge to T1o, and T2oz and T2mo become T2z. For anorthite, the peaks assigned to T1oo and T1mz are over 7 ppm apart, and this separation decreases with increasing Sr content as the peaks merge toward the position of T1o at Sr85. This effect is most clearly observed in the movement of the T1mz peak from −89.5 ppm at Sr0 to −86.7 ppm at Sr80, and in the intensity increase of the peak near −86.0 ppm from Sr80 to Sr85, marking the convergence of peaks for T1oo and T1mz to the *I*2/*c* equivalent, T1o. (Strictly speaking, the Sr0 sample displays local $P\bar{1}$ symmetry at room temperature, as discussed above, with the transition to $I\bar{1}$ occurring at some higher temperature. Although the peak at −89.5 ppm contains signal from both T1mzi and T1mzo, no splitting is evident, and we take its position to be that for T1mz in the $I\bar{1}$ phase.)

The order parameter representing the departure of the $I\bar{1}$ samples from *I*2/*c* symmetry can be determined from the difference in the ^{29}Si NMR chemical shift of a site in the $I\bar{1}$ phase and that of its *I*2/*c* equivalent. The analysis is similar to that described by Phillips and Kirkpatrick (1995) for the $P\bar{1} \rightarrow I\bar{1}$ transition that occurs in pure

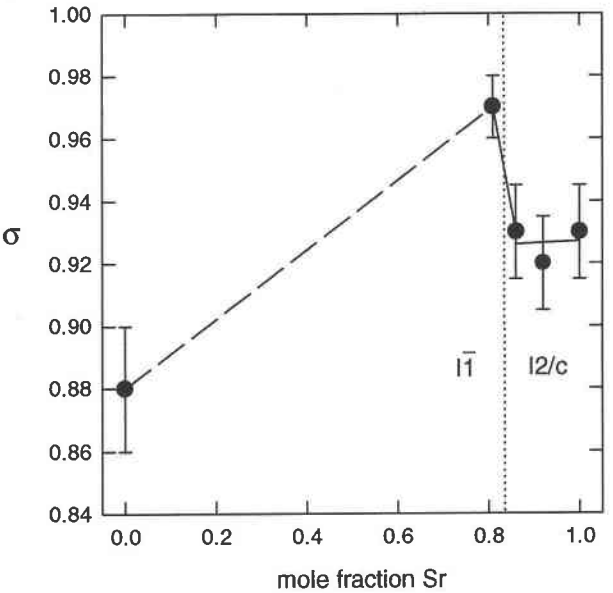

FIGURE 3. Behavior of the order parameter for short-range Si-Al order, σ, across the solid solution. Error bars are estimated uncertainties.

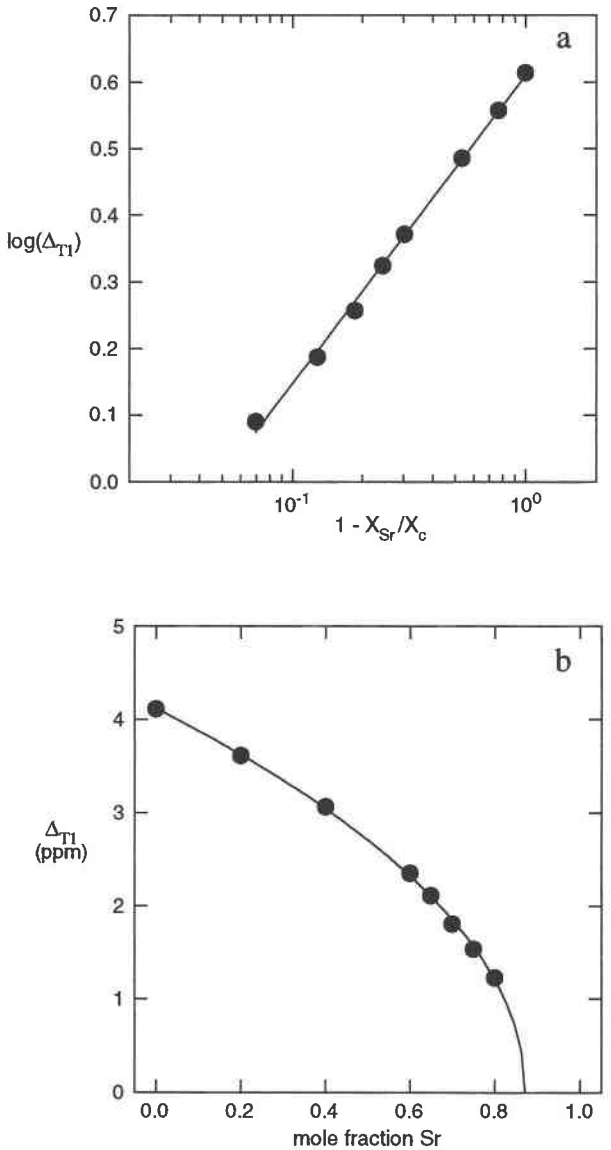

FIGURE 4. Composition dependence of the difference in ^{29}Si NMR chemical shift (Δ_{T_1}) between the peak assigned to T1mz for $I\bar{1}$ samples and that assigned to T1o in the *I*2/*c* phase. (**a**) Log-log plot with reduced composition; critical composition X_c = 0.86 taken from XRD results (McGuinn and Redfern 1994). Linear relationship indicates $\Delta_{T_1} \propto Q$ (Eq. 4), and its slope corresponds to critical exponent, β = 0.46. (**b**) Line is a least-squares fit to Equations 4 and 5, giving β = 0.49(2) and X_c = 0.87(3).

anorthite with increasing *T*. For the present case, quantitative information can be obtained most reliably from the position of the T1mz peak because it is clearly resolved at all compositions and the equivalent peak in the monoclinic samples shows very little compositional dependence.

The difference in chemical shift (Δ_{T_1}) between T1mz and the equivalent *I*2/*c* site, T1o, can be described by a power series of the order parameter, *Q*:

$$\Delta_{T1} = \sum_{i=1}^{n} A_i Q^i \quad (4)$$

with coefficients independent of composition. We assume the simplest form for the variation of the order parameter with composition according to a Landau-type model:

$$Q = (1 - X/X_c)^{\beta} \quad (5)$$

where X_c corresponds to the critical composition, as mole fraction Sr, and β is the order-parameter critical exponent, which would be 0.5 for a second-order transition, or 0.25 if it is tricritical.

The linear covariation of the logarithms of Δ_{T_1} and reduced composition (X/X_c), computed using the value X_c = 0.86 determined from XRD data, indicates that, to a good approximation, $\Delta_{T_1} \propto Q$ (Fig. 4a). Therefore, the first-order approximation for Equation 4 (n = 1) appears adequate. The slope of the best-fit line, 0.46, corresponds to the value of β, assuming X_c = 0.86. A least-squares fit to Equations 4 and 5 gives β = 0.49(2), X_c = 0.87(3), and A_1 = 4.12(4) ppm (Fig. 4b). The root-mean-square residual, 0.02 ppm, is of the order of measurement uncertainty. Although Equations 4 and 5 assume, arbitrarily, that the composition X = 0.0 corresponds to the fully ordered state, fits to the data that incorporate a renormalization of the composition give Q = 1 at X = 0.015 and do not result in significantly different fitted parameters. The best-fit value X_c = 0.87 ± 0.03 is slightly higher than would be consistent with the apparent local *I*2/*c* symmetry displayed by Sr85. Monoclinic symmetry for this sample is suggested by the constant position of the T1o peak from Sr85 to Sr100, in comparison with the strong dependence of the equivalent $I\bar{1}$ peaks on the order parameter. This result is supported by variable-temperature NMR spectra of Sr85, which show no change from 25 to 150 °C (Phillips, unpublished results). Imposition of the constraint $X_c < 0.85$ leads to a slightly poorer fit (root-mean-square deviation 0.06) and a lower value of β (0.45).

Within uncertainty, these NMR results are consistent with a classical second-order $I\bar{1}$-*I*2/*c* transition and are in good agreement with the analysis of the e_4 strain component measured by XRD techniques, which gives β = 0.40 and X_c = 0.86 (McGuinn and Redfern 1994). However, the XRD data show a pronounced strain tail near X_c, including significant triclinic strain for the Sr85 sample, which exhibits local monoclinic symmetry according to our interpretation of the NMR data. For Sr85, the strain correlates with an increase in the width of the T1o peak to 2.3 ppm (FWHM), in comparison with 1.6 ppm for Sr100, whereas the peak position and intensity remain constant. This peak broadening could be due to a small, unresolved triclinic splitting. Deconvolution of the Sr85 and Sr95 T1o peaks with a natural line width corresponding to that observed for Sr100 (1.6 ppm) indicates that the increase of peak width is equivalent to a normal distribution of Q with a width of about 0.15 (1σ) for Sr85, decreasing to about one-half this value for Sr95. How-

ever, peak broadening can also arise from local structural fluctuations resulting from the Ca-Sr distribution. For example, a similar increase in peak width was found for intermediate members of an Na-K series of $C\bar{1}$ feldspar (Phillips et al. 1988). That the preliminary variable-T data show no change in the peak width with increasing T is consistent with the latter interpretation, but the results are not conclusive.

Finally, we note that high-T ^{29}Si NMR spectra of Si-Al–ordered $I\bar{1}$ anorthite, presented by Phillips and Kirkpatrick (1995), also show the effects of an approach toward monoclinic symmetry. With increasing T from 250 to 500 °C the separation of the T1oo and T1mz peaks decreases approximately linearly by 0.4 ppm, equivalent to the change observed in the present study with increasing Sr content from Sr0 to about Sr20. Assuming a second-order transition, extrapolation of the high-T NMR data gives $T_c = 2800 \pm 200$ K for the triclinic-monoclinic transition in pure anorthite. Although this is a very long extrapolation, we note that (1) the fitted value of the coefficient, $A_1 = 3.9$ ppm, is similar to that determined for the strontium-calcium feldspar samples, as would be expected if the coupling coefficients depend only on geometrical factors (e.g., variation of chemical shift with mean Si-O-Al angle), and (2) the transition temperature is of the order of that obtained by Carpenter (1992), on the basis of extrapolations of the $C2/m \rightleftharpoons C\bar{1}$ phase boundary and $\cos^4\alpha^*$. These results, together with those for the Ca-Sr series, demonstrate the sensitivity of NMR chemical shifts to structural changes in feldspar and their usefulness for the measurement of order parameters.

Acknowledgments

We thank Raymond Ward for the use of the NMR spectrometer at Lawrence Livermore National Laboratory (LLNL). Support for B.L.P. during the initial stages of this project was provided by the postdoctoral research program in the Earth Sciences Division of LLNL. M.D.M. and S.A.T.R. are grateful for the financial support of the Nuffield Foundation and NERC. Helpful comments from Torsten Schaller and an anonymous reviewer led to improvements in the manuscript.

References cited

Carpenter, M.A. (1992) Equilibrium thermodynamics of Al/Si ordering in anorthite. Physics and Chemistry of Minerals, 19, 1–24.

Chiari, G., Calleri, M., Bruno, E., and Ribbe, P.H. (1975) The structure of partially disordered, synthetic strontium feldspar. American Mineralogist, 60, 111–119.

Dove, M.T., and Redfern, S.A.T. (1997) Lattice simulation studies of the ferroelastic phase transitions in disordered $(Na,K)AlSi_3O_8$ and ordered $(Sr,Ca)Al_2Si_2O_8$ feldspar solid solutions. American Mineralogist, 82, 8–15.

McGuinn, M.D., and Redfern, S.A.T. (1994) Ferroelastic phase transition along the join $CaAl_2Si_2O_8$-$SrAl_2Si_2O_8$. American Mineralogist, 79, 24–30.

Phillips, B.L., Kirkpatrick, R.J., and Hovis, G.L. (1988) ^{27}Al, ^{29}Si, and ^{23}Na MAS NMR study of an Al,Si ordered alkali feldspar series. Physics and Chemistry of Minerals, 16, 262–275.

Phillips, B.L., Kirkpatrick, R.J., and Carpenter, M.A. (1992) Investigation of short-range Al,Si order in synthetic anorthite by ^{29}Si MAS NMR spectroscopy. American Mineralogist, 77, 484–494.

Phillips, B.L., and Kirkpatrick, R.J. (1995) High-temperature ^{29}Si MAS NMR spectroscopy of anorthite and its $P\bar{1}$-$I\bar{1}$ structural phase transition. Physics and Chemistry of Minerals, 22, 268–276.

Radeglia, R., and Engelhardt, G. (1985) Correlation of Si-O-T (T = Si or Al) angles and ^{29}Si NMR chemical shifts in silicates and aluminosilicates: Interpretation by semi-empirical quantum-chemical considerations. Chemical Physics Letters, 114, 28–30.

Salje, E., Kuscholke, B., Wruck, B., and Kroll, H. (1985) Thermodynamics of sodium feldspar: II. Experimental results and numerical calculations. Physics and Chemistry of Minerals, 12, 99–107.

Tribaudino, M., Benna, P., and Bruno, E. (1993) $I\bar{1}$-$I2/c$ phase transition in alkaline earth feldspars along the $CaAl_2Si_2O_8$-$SrAl_2Si_2O_8$ join: Thermodynamic behaviour. Physics and Chemistry of Minerals, 20, 221–227.

——— (1995) $I\bar{1}$-$I2/c$ phase transition in alkaline-earth feldspars: Evidence from TEM observations of Sr-rich feldspars along the $CaAl_2Si_2O_8$-$SrAl_2Si_2O_8$ join. American Mineralogist, 80, 907–915.

Manuscript received January 2, 1996
Manuscript accepted September 24, 1996